Article

Structure of *Petunia hybrida* Defensin 1, a Novel Plant Defensin with Five Disulfide Bonds

Bert J. C. Janssen, Horst Joachim Schirra, Fung T. Lay, Marilyn A. Anderson, and David J. Craik

More About This Article

Additional resources and features associated with this article are available within the HTML version:

- Supporting Information
- Links to the 4 articles that cite this article, as of the time of this article download
- Access to high resolution figures
- Links to articles and content related to this article
- Copyright permission to reproduce figures and/or text from this article

View the Full Text HTML

ACS Publications
High quality. High impact.

Structure of *Petunia hybrida* Defensin 1, a Novel Plant Defensin with Five Disulfide Bonds[†]

Bert J. C. Janssen,[‡] Horst Joachim Schirra,[‡] Fung T. Lay,[§] Marilyn A. Anderson,[§] and David J. Craik*[,‡]

Institute for Molecular Bioscience, ARC Special Research Center for Functional and Applied Genomics, The University of Queensland, Brisbane, Queensland 4072, Australia, and Department of Biochemistry, La Trobe University, Bundoora, Victoria 3086, Australia

ABSTRACT: The structure of a novel plant defensin isolated from the flowers of *Petunia hybrida* has been determined by ^{1}H NMR spectroscopy. *P. hybrida* defensin 1 (PhD1) is a basic, cysteine-rich, antifungal protein of 47 residues and is the first example of a new subclass of plant defensins with five disulfide bonds whose structure has been determined. PhD1 has the fold of the cysteine-stabilized $\alpha\beta$ motif, consisting of an α-helix and a triple-stranded antiparallel β-sheet, except that it contains a fifth disulfide bond from the first loop to the α-helix. The additional disulfide bond is accommodated in PhD1 without any alteration of its tertiary structure with respect to other plant defensins. Comparison of its structure with those of classic, four-disulfide defensins has allowed us to identify a previously unrecognized hydrogen bond network that is integral to structure stabilization in the family.

Antimicrobial proteins play an important role in the defense mechanisms of eukaryotes (*1*). In plants, they constitute a part of the molecular defense arsenal that includes various other antimicrobial substances such as hydrogen peroxide and phytoalexins (*2*, *3*). Antimicrobial proteins are widely distributed throughout the plant kingdom and can be grouped into several families based on their primary structure. They include thionins, lipid transfer proteins, heveins, knottins, and plant defensins (*2*).

Plant defensins are a family of highly stable, basic proteins of 45−54 amino acids, containing eight cysteine residues that form four disulfide bridges (*4*). Members of this family have been characterized in several plant species at both the DNA and protein level from various plant tissues, including leaves, pods, tubers, fruit, and flowers (*2*, *5*) (Figure 1). Much of the work, however, has been performed on seeds where these proteins are prevalent (*6*).

It is not known whether plant defensins have a common mode of action. However, Rs-AFP2, one of the best-characterized antifungal plant defensins, has been suggested to interact with a membrane-bound receptor rather than by permeabilizing the membrane by direct defensin−lipid interaction (*7*).

All plant defensins share a characteristic three-dimensional folding pattern, stabilized by four disulfide bridges (*4*), that incorporates the cysteine-stabilized $\alpha\beta$ (CS$\alpha\beta$)[1] motif (*8*).

The three-dimensional structure is dominated by a triple-stranded, antiparallel β-sheet and a single α-helix lying in parallel with the β-sheet (*9*). The α-helix is connected by two disulfide bridges to the central β-strand (β3) of the antiparallel β-sheet; strand β2 is connected by a disulfide bridge to the first loop, and the N- and C-termini are connected by a disulfide bridge. The plant defensins are structurally related to insect and mammalian defensins except that insect defensins contain three disulfide bridges and lack the region corresponding to the amino-terminal β-strand of plant defensins, while the mammalian defensins contain a triple-stranded antiparallel β-sheet stabilized by three disulfide bonds but lack the CS$\alpha\beta$ motif (*4*).

PhD1 and PhD2 are two recently discovered defensins from the flowers of *Petunia hybrida* (*10*). Their sequences are shown in Figure 1. They are the first described plant defensins containing five disulfide bonds. PhD1 inhibits the growth of the fungi *Botrytis cinerea* and *Fusarium oxysporum f. sp. dianthi* and may thus be of interest for the development of novel fungicides (*10*).

Among the plant defensins with four disulfide bonds, the protein with the sequence most identical to those of PhD1 and PhD2 is the *Nicotiana alata* plant defensin NaD1, the sequence of which is 51 and 72% identical, respectively (*5*). Apart from the cysteines, key residues conserved in

* To whom correspondence should be addressed: Institute for Molecular Bioscience, The University of Queensland, Brisbane, Qld 4072, Australia. Telephone: 61-7-33462019. Fax: 61-7-33462101. E-mail: d.craik@imb.uq.edu.au.

‡ The University of Queensland.

§ La Trobe University.

[1] Abbreviations: Rs-AFP2, *Raphanus sativus* antifungal protein 2; CS$\alpha\beta$, cysteine-stabilized $\alpha\beta$; PhD1, *P. hybrida* defensin 1; PhD2, *P. hybrida* defensin 2; NaD1, *N. alata* defensin 1; NMR, nuclear magnetic resonance; RP-HPLC, reverse-phase high-pressure liquid chromatography; TPPI, time-proportional phase incrementation; DQF-COSY, double-quantum-filtered correlated spectroscopy; NOESY, nuclear Overhauser enhanced spectroscopy; TOCSY, total correlation spectroscopy; E.COSY, exclusive COSY; HSQC, heteronuclear single-quantum coherence; Rs-AFP1, *R. sativus* antifungal protein 1; CSH, cysteine-stabilized α-helix; Ah-AMP1, *Aesculus hippocastanum* antimicrobial protein 1; Psd1, *Pisum sativum* defensin 1.
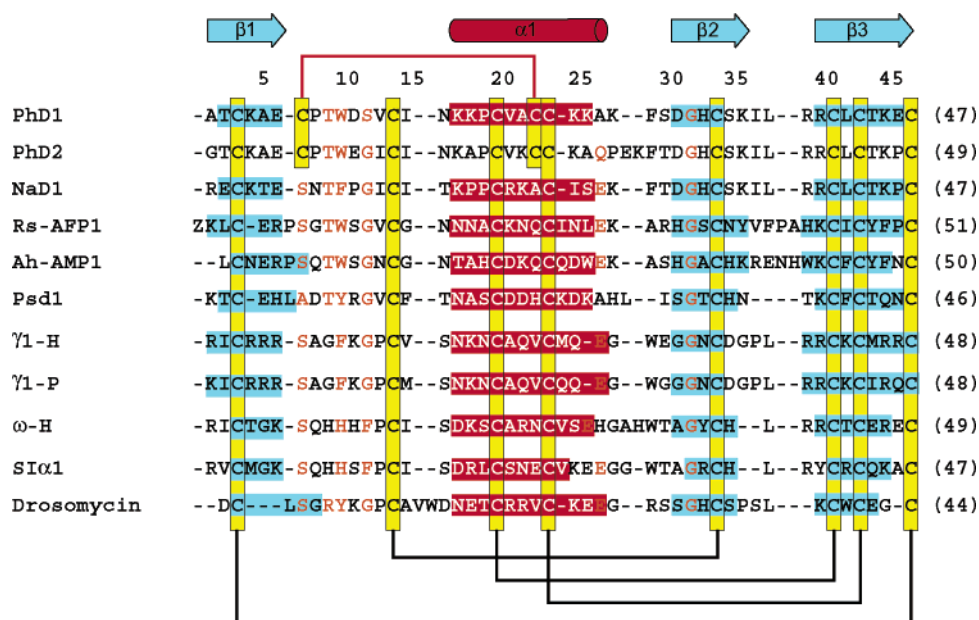
FIGURE 1: Sequence alignment of PhD1 and PhD2 with plant defensins NaD1 (*5*), Rs-AFP1 (*32*), Ah-AMP1 (*35*), Psd1 (*36*), γ1-H and γ1-P (*9*), ω-H (*40*), and SIα1 (*41*), and with the antifungal drosomycin from *Drosophila melangogaster* (*37*). Gaps have been introduced to maximize sequence similarity. Amino acid residues are numbered above the sequences, according to the PhD1 sequence. The length of each protein is indicated in parentheses next to the sequence. Z is the one-letter code for pyroglutamic acid. α-Helices and β-strands are indicated above the sequences and by red and blue shading, respectively, within the sequences. The cysteine residues are highlighted by yellow rectangles, and the disulfide bonds are depicted by connecting lines. The fifth disulfide bond of PhD1 is indicated by a red line. Conserved residues are highlighted in orange.

almost all plant defensins are a serine at position 7, an aromatic residue at position 10, two glycines at positions 12 and 32, and a glutamic acid at position 27 (numbering relative to NaD1) (*4*, *5*). In PhD1, however, Ser7 is replaced with a cysteine, Gly12 is replaced with a serine residue, and Glu27 is replaced with an alanine (Figure 1).

Here we describe the solution structure of PhD1, as determined by ^{1}H NMR spectroscopy. This represents the first reported structure of a plant defensin containing five disulfide bridges. PhD1 has a compact three-dimensional structure and possesses all the characteristics of the CSαβ motif. We compare the region of the additional disulfide bond in PhD1 with other plant defensins to gain insight into the functional significance of this new structural feature. This analysis reveals a previously undescribed network of hydrogen bonds, which is likely to be conserved in most plant defensins and is important in the stabilization of the plant defensins.

MATERIALS AND METHODS

Purification of PhD1

PhD1 was isolated and purified as described by Lay et al. (*10*). Mass spectrometry confirmed that all 10 cysteines in PhD1 were in the oxidized form. RP-HPLC and NMR studies confirmed that the protein is >95% pure.

NMR Spectroscopy

General Conditions. Samples for NMR spectroscopy contained 0.94 mM PhD1 in either a 90% H_2O/10% D_2O mixture or 99% D_2O at pH 3.1. The protein is monomeric under these conditions, as judged by the line width of the NMR signals. Spectra were recorded at 280 and 310 K on a Bruker DMX750 spectrometer with a 5 mm triple-resonance self-shielded z-gradient probe. Quadrature detection in the

indirect dimensions was achieved using the TPPI method (*11*). The spectral width was 10 ppm for ^{1}H, and the carrier frequency was positioned on the water resonance. Water suppression in the DQF-COSY experiments was achieved using selective low-power irradiation of the water resonance during a relaxation delay of 1.3 s. For NOESY and TOCSY experiments, a 3-9-19 WATERGATE scheme (*12*) was used, employing gradient pulses of 6 G/cm on either side of a 10 kHz 3-9-19 binomial pulse. TOCSY experiments used the MLEV17 sequence (*13*) for isotropic mixing. The same pulse sequences were used for measurements in D_2O, except that no water suppression was necessary.

Data Acquisition. The following spectra were recorded for PhD1 in a 90% H_2O/10% D_2O mixture: DQF-COSY (*14*) with 4096 × 512 data points, two-dimensional (2D) TOCSY (*15*) with a spin-lock time of 80 ms and 4096 × 512 data points, and 2D NOESY (*16*) with mixing times of 150, 250, and 400 ms and 4096 × 512 data points. No signs for spin diffusion were found in the spectra at 150 and 250 ms. Slowly exchanging amide protons were identified by recording a series of TOCSY and one-dimensional (1D) spectra at 310 K on a fully protonated sample of PhD1 immediately after dissolution in D_2O. The following spectra were recorded on PhD1 in 99.9% D_2O: TOCSY with a mixing time of 80 ms and 4096 × 512 data points, 2D E.COSY (*17*) with 4096 × 512 data points, and 2D NOESY (*16*) with mixing times of 150 and 250 ms and 4096 × 512 data points. A ^{13}C HSQC spectrum (*18*) with 4096 × 280 data points was recorded at natural abundance on PhD1. The spectral width in the carbon dimension was 80 ppm, and the carrier frequency was positioned at 35 ppm.

Data Processing. Spectra were processed on an SGI Octane R12000 workstation using XWINNMR (Bruker). Data were analyzed using the program GLXCC (*19*).

Resonance Assignments

The NMR spectra of PhD1 exhibited good chemical shift dispersion in the amide region, indicating a well-defined structure under the conditions of the NMR experiments. The resonances of PhD1 were assigned using homonuclear two-dimensional NMR methods (20). In the initial 2D spectra, it was not possible to determine whether both prolines were in the *cis* or *trans* conformation due to the overlap of several crucial resonances in the homonuclear NOESY spectrum. For the connection between Cys7 and Pro8, one of the Pro8 H^δ resonances has the same chemical shift as the Cys7 H^α signal. For the Lys18−Pro19 connection, the resonance of Pro19 H^α is close to the water signal and has the same chemical shift as the Ser35 H^α resonance, while the signal of Lys18 H^α overlaps with both H^β signals of Ser35. Analysis of a ^{13}C HSQC spectrum, recorded at natural abundance, showed that the difference in the ^{13}C chemical shift between the C^β and C^γ resonances of the prolines is 5 ppm for Pro8 and 2.5 ppm for Pro19. Previous studies have shown that the $C^\beta−C^\gamma$ separation is generally ∼5 ppm for *trans* Xaa− Pro bonds and ∼10 ppm for *cis* Xaa−Pro bonds (21). Thus, both proline residues of PhD1 are in the *trans* conformation. This was confirmed by a second analysis of homonuclear NOESY spectra recorded at different temperatures.

Distance Constraints and Structure Calculations

Four hundred seven distance constraints were derived from 250 and 150 ms mixing time NOESY spectra recorded in a 90% H_2O/10% D_2O mixture or in 99.9% D_2O as described previously (22). Upper limits of 1.0, 1.5, and 2.0 Å were added for non-stereospecifically assigned methylene, methyl, and phenyl ring protons, respectively (20). $^3J_{HNH\alpha}$ coupling constants and a comparison of intraresidual $H^N(i)−H^\alpha(i)$ NOEs with sequential $H^N(i + 1)−H^\alpha(i)$ NOEs were used to determine a total of 26 ϕ angle constraints (23). $^3J_{H\alpha H\beta}$ coupling constants in conjunction with relevant NOE intensities, from the NOESY spectra with a mixing time of 150 or 250 ms, were used to determine 28 χ_1 angle constraints (24). Initial structures were calculated using XPLOR version 3.851 (25). Several rounds of structure calculations were performed to resolve ambiguities in the assignment of NOE cross-signals. Hydrogen bond constraints of 1.9−2.2 Å between donor H^N and acceptor O′ atoms, and of 2.7−3.0 Å between donor N and acceptor O′ atoms, were added, where the correct hydrogen bonding geometry could be determined from structure calculations without hydrogen bond constraints and where the H^N proton had been identified as a slowly exchanging proton in the $H_2O−D_2O$ exchange experiments (20). A total of 30 constraints, representing 15 hydrogen bonds, was added in this way.

A final set of 50 structures was calculated using the standard torsion angle simulated annealing protocol incorporated within the program CNS (26) and afterward refined in a box with explicit water molecules using the method of Linge and Nilges (27).

A total of 20 structures with the lowest overall energy that had no violations of distance restraints greater than 0.25 Å and no violations of dihedral angles greater than 3.0° was chosen to represent the structure of PhD1. Structures were visualized using the program MOLMOL (28) and analyzed with PROMOTIF (29) and PROCHECK-NMR (30).

Coordinates

The 20 final structures of PhD1 and the restraints used to generate them have been deposited in the Protein Data Bank as entry 1n4n (RCSB entry 017513).

RESULTS

Secondary Structure of PhD1. Sequential and medium-range NOEs observed in the NOESY spectra of PhD1 were the basis for the determination of the secondary structure of PhD1 (Figure 2). The dominant structural features of PhD1 are a triple-stranded antiparallel β-sheet and an α-helix. The primary evidence for the antiparallel β-sheet structure is the presence of several intrastrand $H^N(i)−H^\alpha(i − 1)$ NOEs as well as several characteristic interstrand $H^N(i)−H^N(j)$, $H^N(i)−H^\alpha(j)$, and $H^\alpha(i)−H^\alpha(j)$ NOEs (20) (Figure 2). This is supported by the observation of several slowly exchanging H^N protons and large (>9 Hz) $^3J_{HNH\alpha}$ coupling constants within the β-sheet (Figure 2). Residues Cys41−Glu46 form the central strand (β3) of the β-sheet, while residues Thr2− Glu6 (β1) and residues Asp31−Cys34 (β2) form the two peripheral strands. In addition to the β-sheet, an α-helix was identified from residue Lys17 to Lys26 by the presence of $H^N(i)−H^N(i + 1)$, $H^N(i)−H^N(i + 2)$, $H^\alpha(i)−H^N(i + 3)$, and $H^\alpha(i)−H^N(i + 4)$ NOEs (20). This was supported by the observation of slowly exchanging H^N protons for residues within the α-helix (Figure 2).

Tertiary Structure. The three-dimensional structure of PhD1 was calculated from a total of 407 interresidual distance constraints derived from 165 sequential, 82 medium-range, and 160 long-range NOEs together with 26 ϕ and 28 χ_1 dihedral constraints. No intraresidual distance constraints were used. At a later stage of the structure calculations, 30 hydrogen bonds constraints (defining 15 hydrogen bonds) were added for slowly exchanging amide protons where the acceptor carbonyl groups could be determined from previous calculations without these constraints.

A total of 50 structures was generated using a simulated annealing method within the program CNS (26). The 20 structures with the lowest energies that had no violations of distance restraints greater than 0.25 Å and no violations of dihedral angles greater than 3.0° were chosen to represent the solution structure of PhD1. Figure 3A shows the ensemble of structures superimposed over the backbone heavy atoms of residues involved in secondary structure elements (2−6, 17−26, 31−34, and 41−46). All structures satisfy the experimental constraints with only minor deviations from idealized covalent geometry (Table 1). The backbone rmsd of the 20 refined PhD1 structures is 0.32 Å for residues involved in secondary structure elements and 0.57 Å for all residues. The rmsd value over the entire molecule is 1.22 Å for heavy atoms and 1.64 Å for all atoms.

PhD1 adopts a very compact globular fold (Figure 3B). The β-sheet is regular, with strand β1 at an angle of 31° relative to strand β3, and the angle between strand β3 and strand β2 is 29°. The α-helix extends 15 Å and spans 10 residues from Lys17 to Lys26 (three helical turns), which is evidenced by an abrupt change in ϕ and ψ dihedral angles at the residues preceding Lys17 and following Lys26. The values of the dihedral angles for the Lys17−Lys26 fragment are within 20° of the values of the regular α-helix (−57° and −48° for ϕ and ψ, respectively). Only the backbone
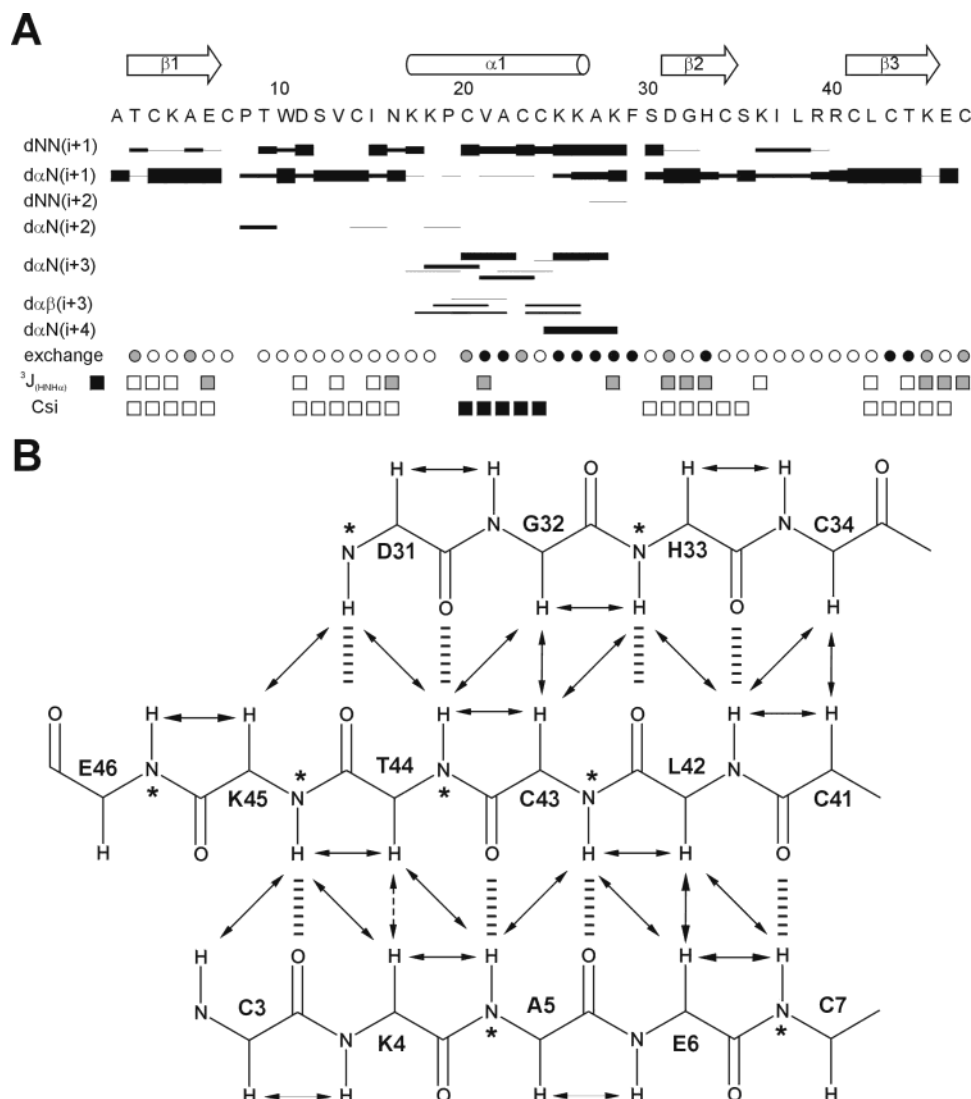
FIGURE 2: Identification of the secondary structure elements of PhD1. (A) Amino acid sequence of PhD1 and survey of NMR data used to identify regular secondary structure. The sequential and medium-range NOEs ($|i − j| < 5$) are represented by lines connecting the two residues related by the NOE. NOE intensities, grouped into five classes, are represented by the heights of bars. The $H^\alpha(H^N)(i)−H^\delta(i + 1)$ NOEs of proline residues are shown along the same line as the $H^\alpha(H^N)(i)−H^N(i + 1)$ connectivities. Filled circles below the amino acid sequence indicate the positions of amide protons that exchange sufficiently slowly to be observed in TOCSY spectra 12 h after dissolving a lyophilized protein sample in D_2O at 298 K. Amide protons fully exchanged after 1 h are indicated by empty circles, while amide protons with intermediate exchange behavior are indicated by gray circles. The values of the $^3J_{HNH\alpha}$ coupling constants (in Hertz) are indicated by gray ($J < 7$ Hz) and empty ($J > 7$ Hz) squares. The chemical shift index (CSI) (*42*) is also indicated below the sequence with filled and empty squares designating α-helices and β-sheets, respectively. The arrows and helices at the top of the figure indicate the position of regular secondary structure elements in PhD1 as identified from the calculated structures. (B) Triple-stranded antiparallel β-sheet region in PhD1 showing the interstrand NOEs (arrows), hydrogen bonds (dashed lines), and slowly exchanging H^N protons (asterisks). Interstrand NOEs, which could not be observed due to overlap, are represented by dashed arrows.

dihedral angles of Ala27 have values more characteristic of a 3_{10}-helix ($\phi = −86°$, $\psi = 4°$). The H^N atoms of Lys28 and Phe29 have hydrogen bonds to the carbonyl oxygen atoms of Lys25 and Cys24, respectively, forming a classical non-glycine Schellmann motif for C-capping. The backbone of Asn16 has a β-conformation, which is regularly observed for an N-capping asparagine (*31*). The side chain carbonyl atom of Asn16 acts as a hydrogen bond acceptor for the H^N of Lys18, while the O′ of Cys20 maintains a hydrogen bond with the main chain H^N of Asn16 in a modified N-capping box. A similar arrangement has also been observed in the radish plant defensin Rs-AFP1 (*32*).

The tertiary structure of PhD1 has the general fold of the cysteine-stabilized αβ (CSαβ) motif (*8*), which elaborates on a smaller motif known as the cysteine-stabilized α-helix

(CSH) motif (*33*). The CSH motif consists of a pair of cysteines, located on an α-helix and separated by three amino acids (CXXXC). This pair of cysteines is connected via two disulfide bridges to a second pair of cysteines which is located on the middle strand of an antiparallel β-sheet and separated by one amino acid (CXC). This consensus sequence is expanded in the CSαβ motif to include a third disulfide bond, which connects the loop between strands β2 and β3 with an extended loop between strand β1 and the α-helix. The consensus sequence of the CSαβ motif can be represented as C^1-$(X)_i$-C^2XXXC^3-$(X)_j$-$C^{1'}$-$(X)_k$-$C^{2'}XC^{3'}$, and the CSαβ motif is incorporated in PhD1 in the following form: Cys14 for C^1, Cys20 for C^2, Cys24 for C^3, Cys34 for $C^{1'}$, Cys41 for $C^{2'}$, and Cys43 for $C^{3'}$. In addition to the CSαβ motif, a fourth pair of cysteine residues (Cys3−Cys47
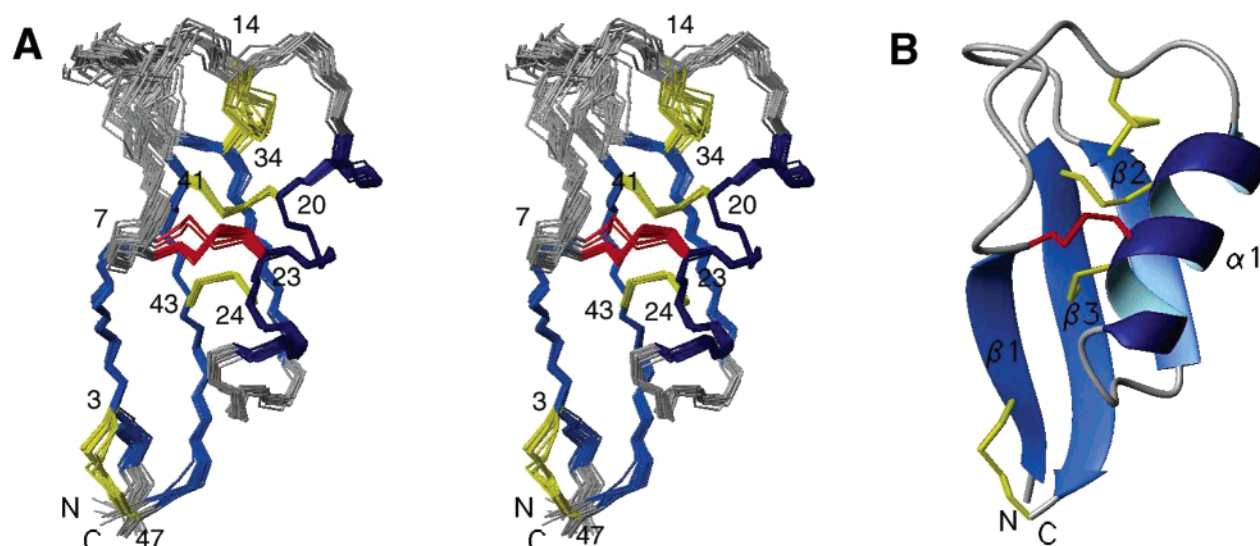
FIGURE 3: (A) Stereoview of the backbone atoms of all residues for the family of the 20 structures of PhD1 best fitted to N, C$^\alpha$, and C′ atoms of residues in secondary structure elements (residues 2−6, 17−26, 31−34, and 41−46). The four disulfide bonds, common to all plant defensins, are colored yellow; the fifth disulfide bond, which is unique to PhD1, is colored red. (B) Ribbon representation of the model with the lowest energy of the solution structure of PhD1, showing the regular secondary structure and global fold of the protein. The N- and C-termini as well as all secondary structure elements are indicated. The side chains of the five disulfide bonds are shown explicitly and are colored yellow; the fifth disulfide bond, which is unique to PhD1, is colored red. The orientation of PhD1 as shown in the figure is a standard orientation that is maintained in most of the figures in this paper. This figure was produced with MOLMOL (*28*).

Table 1: Parameters Characterizing the Structure Determination of PhD1

parameter	$\langle PhD1 \rangle^a$
energy (kcal/mol)	
total	−1793.52 ± 58.41
bond lengths	9.84 ± 1.34
bond angles	52.55 ± 7.39
impropers	9.84 ± 1.91
van der Waals	−121.53 ± 13.55
restraint violations	11.05 ± 2.70
dihedral angles	0.77 ± 0.43
electrostatic	−1957.32 ± 73.79
no. of residual constraint violations	
for all distance constraints	
0.2 Å < rmsd < 0.25 Å	0.30 ± 0.47
>0.25 Å	0
deviation from idealized geometry	
bond lengths (Å)	0.004 ± 0.000
bond angles (deg)	0.509 ± 0.034
improper angles (deg)	0.424 ± 0.039
rmsd from experimental distance constraints	
NOEs (Å)	0.023 ± 0.029
dihedral angle restraints (deg)	0.469 ± 0.133
Ramachandran statistics (%)	
residues in most favored regions	81.5
residues in additional allowed regions	18.2
residues in generously allowed regions	0.2
residues in disallowed regions	0.0

^{a} $\langle PhD1 \rangle$ represents the ensemble of the 20 final structures. The structures were calculated using a torsion angle simulated annealing and energy minimization protocol in CNS (*26*). The resulting structures were refined in a box of explicit water molecules using the method of Linge and Nilges (*27*).

in PhD1) is highly conserved among plant defensins and forms a disulfide bond between the N- and C-termini [cf. the PROSITE (*34*) signature (PS00940) for γ-thionins]. PhD1 is the first defensin with an extra cysteine pair (Cys7−Cys23) that forms a fifth disulfide bond from the α-helix to the loop between strand β1 and the α-helix. Because of the presence of these five disulfide bridges, the structure of PhD1 is very compact.

The loop between strand β1 and the α-helix (Ser7−Asn16) is stabilized by the aromatic side chain of Trp10, in addition to the two disulfide bridges (Cys3−Cys23 and Cys14−Cys34). The loop wraps around the side chain of Trp10 and is stabilized by hydrophobic interactions between the indole ring of Trp10 and the backbone atoms of the loop, as evidenced by a number of NOEs between the Trp10 side chain and the loop. Further evidence for the interaction between the side chain of Trp10 and the loop comes from the profound effect that the aromatic indole ring of Trp10 has on the chemical shifts of nuclei in its vicinity. For example, the H$^\beta$ resonances of Cys41 and the H^N resonance of Ser12 experience marked upfield chemical shifts because of the ring current of the indole ring of Trp10.

Electrostatic Surface Properties of PhD1. PhD1 has two sides with different electrostatic surface characteristics (Figure 4). The side of PhD1 that incorporates the α-helix is predominantly positively charged along the α-helix. Only the C-terminus contains a small negatively charged region formed by Glu46. The other side of PhD1, bearing the β-sheet, is predominantly hydrophobic with only small positively (e.g., Lys4) and negatively charged areas (e.g., Glu6) distributed across the surface.

DISCUSSION

PhD1 is the first defensin from *P. hybrida* to be structurally characterized and the first member of a new subclass of plant defensins that contain five disulfide bonds. The three-dimensional structure of PhD1 features all the characteristics of the CS$\alpha\beta$ motif (*8*) and is dominated by a triple-stranded, antiparallel β-sheet (strand β1 from Thr2 to Glu6, strand β2 from Asp31 to Cys34, and strand β3 from Cys41 to Glu46) and a single α-helix (from Lys17 to Lys26) lying in parallel with the β-sheet. The α-helix is connected by two disulfide bridges to the central strand (β3) of the antiparallel β-sheet; the N- and C-termini are connected by a disulfide bridge, and strand β2 is connected with a disulfide bridge to the
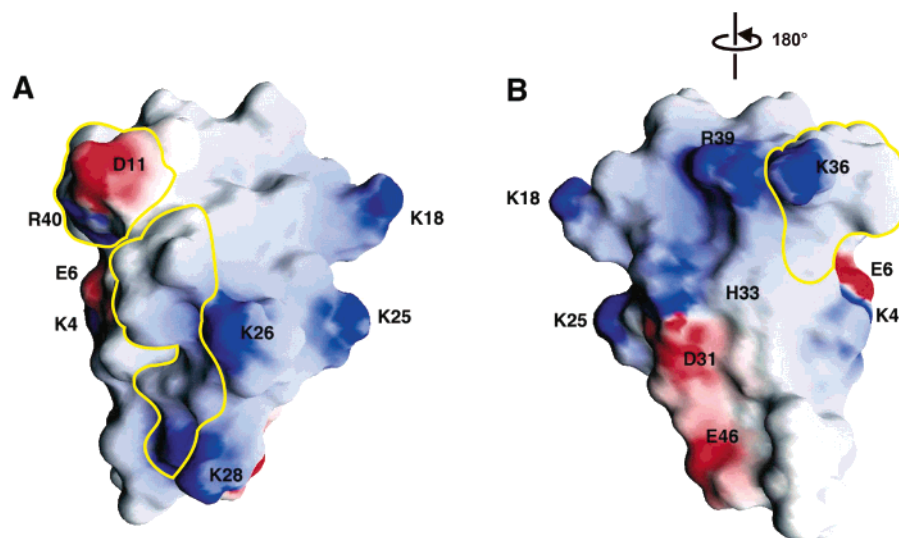
FIGURE 4: Electrostatic surfaces of a representative structure of PhD1. Surfaces are colored by charge (red is negative, blue positive, and white uncharged or hydrophobic). Two surface patches that are potentially involved in the antifungal activity of the protein are indicated by yellow outlines. The molecule is shown in two orientations. (A) PhD1 is oriented with the α-helix in front of the molecule. (B) The molecule is rotated 180° about a vertical axis with the β-sheet in front. This figure was produced with GRASP (*43*).

first loop. In PhD1, the first loop is further connected to the α-helix by a fifth disulfide bond.

The electrostatic surface of PhD1 (Figure 4) provides some insight into the function of the protein. Residues essential for antifungal activity have previously been identified in the plant defensin Rs-AFP2 (*39*). They are located in the loop connecting strands β2 and β3, in the loop connecting strand β1 and the α-helix, and on the α-helix and strand β3 itself. Structurally, they form two adjacent patches on the surface of Rs-AFP2 that are essential for its antifungal activity (*39*). The equivalent residues in the structure of PhD1 also form two patches on the surface of the protein (Figure 4), but their electrostatic character is slightly different from that of Rs-AFP2. In Rs-AFP2, both patches are predominantly uncharged with the exception of Lys44. While the predominant nature of both patches in PhD1 is still uncharged, the contributions of charged residues to these areas are notably larger in PhD1 than in Rs-AFP2, especially toward the "top" of the molecule (β1−α1 and β2−β3 loops) (Figure 4). If plant defensins act by binding to a receptor as has been previously suggested (*7*), then it is tempting to speculate that the receptor for PhD1 may be different from the receptor for Rs-AFP2.

To gain an insight into how the extra disulfide bond is accommodated within the structure of PhD1 and what influence it has on the structure of PhD1 relative to other plant defensins with four disulfide bonds, the structure of PhD1 was compared with the structures of NaD1 (*5*), Rs-AFP1 (*32*), Ah-AMP1 (*35*), γ1-H (*9*), Psd1 (*36*), and drosomycin (*37*).

One possibility is that the extra disulfide bond in PhD1 changes the orientation of the α-helix with respect to the β-sheet. However, a comparison of the angles between the strands of the β-sheet and the α-helix in PhD1 with those of other plant defensins shows that these angles are well within the variation that is already encountered in the different plant defensins that have four disulfide bridges. The distance between the C^α atoms of Cys7 and Cys23, i.e., the two residues connected via the additional disulfide bond, is also about the same size in PhD1 as in the plant defensins with

only four disulfide bridges. It is obvious from this comparison that the additional disulfide bond in PhD1 is incorporated within the structure of PhD1 without a disturbance of the fold of the protein or the orientation of its secondary structure elements.

Another hypothesis is that the extra disulfide bond enhances the stability of the loop between strand β1 and the α-helix. In all known structures of plant defensins, this loop is stabilized by a conserved aromatic residue (Trp10 in PhD1) whose side chain is involved in hydrophobic interactions with the backbone of the loop. The extra disulfide bond in PhD1 does indeed seem to add further to the stability of the loop. The local backbone rmsd values (normalized to the rmsd values within regular secondary structure elements) of the Cys7−Trp10 segment are lower in PhD1 than in most other plant defensins, even in structures where the local backbone rmsd in regions of regular secondary structure is similar to that of PhD1. Apparently, the additional disulfide bond restricts the variability of this part of the loop in PhD1, thus further enhancing its stability.

To assess further contributions of the fifth disulfide bond to the overall stability of the molecule, we compared the region around the disulfide bond in PhD1 with the corresponding regions of other plant defensins, and identified common structural features that are present in these proteins. This structural comparison revealed a previously undescribed hydrogen bond between two semiconserved amino acids that is present in all plant defensins (Figure 5). The hydrogen bond connects the side chain of a charged residue (usually a glutamic acid) at position 27 ("residue A") at the end of the α-helix with the side chain of a semiconserved threonine residue at position 9 ("residue B") on strand β1 (numbers relative to NaD1) (Figure 5, top left and center). The charged residue A is usually located four residues after the second disulfide bond that anchors the α-helix to strand β3 of the β-sheet, while residue B is located directly before the aromatic side chain that stabilizes the β1−α1 loop.

It has previously been observed that in most defensins there is at least one glutamate residue (Glu27 in NaD1) present at the end of the α-helix that may be involved in
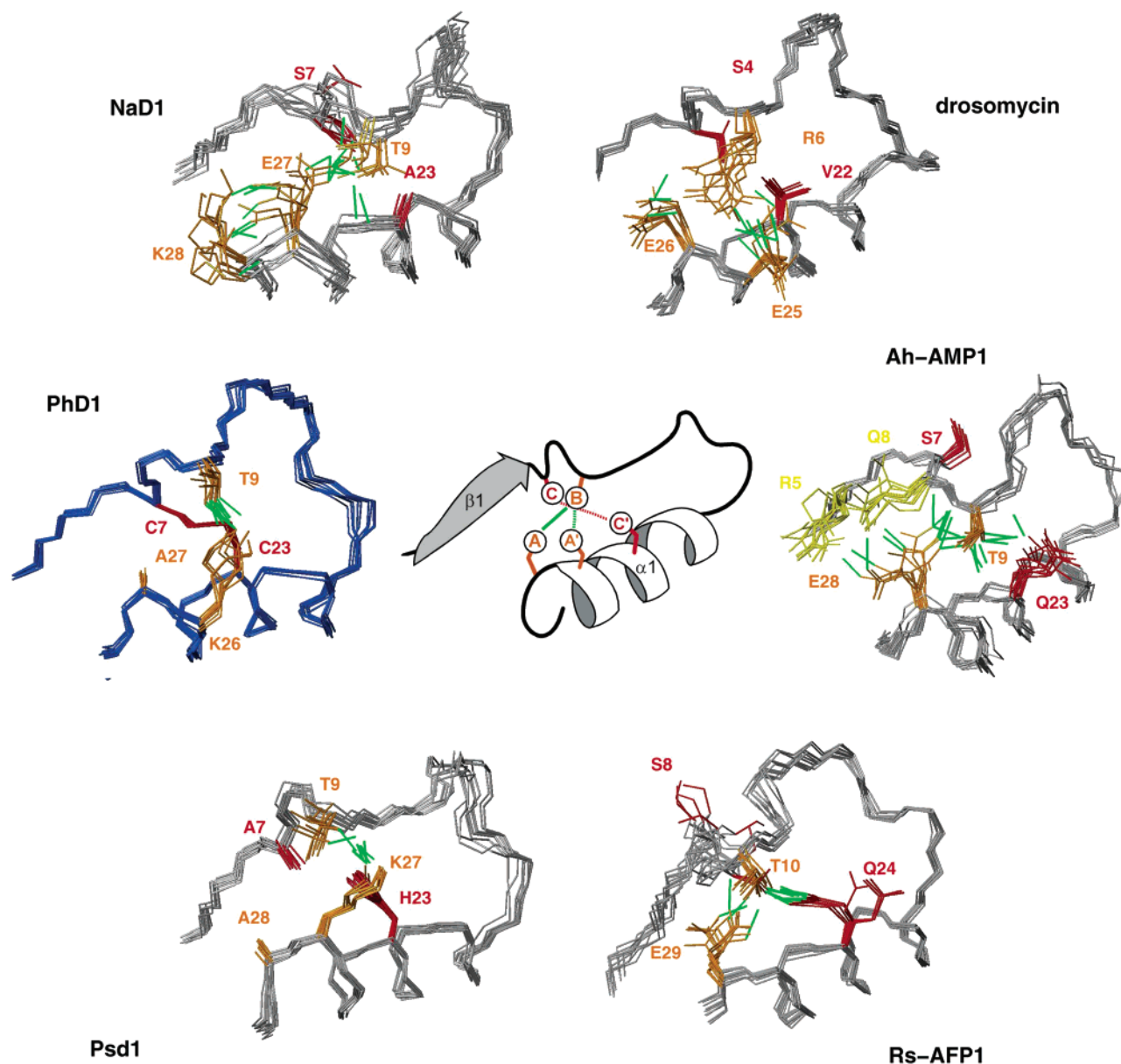
FIGURE 5: Conserved hydrogen bond between the α-helix and strand β1 of plant defensins. Shown are the structural families for NaD1 (*5*) (top left), drosomycin (*37*) (top right), Ah-AMP1 (*35*) (middle right), Rs-AFP1 (*32*) (bottom right), Psd1 (*36*) (bottom left), and PhD1 (blue, middle left). For each protein, the backbone fragment encompassing strand β1 and the α-helix is shown as are the side chains that participate in hydrogen bonds between strand β1 and the α-helix. Conserved side chains A/A′ and B, participating in the conserved hydrogen bond, are colored orange; side chains C and C′, equivalent to the fifth disulfide bond in PhD1, are colored red, and other residues participating in an extended hydrogen bonding network are colored yellow. Hydrogen bonds are represented by green lines. In the center is a schematic drawing of the conserved hydrogen bond. The color coding is similar to that of the individual structure families. The conserved hydrogen bond between A and B or A′ and B is indicated by a solid or dashed green line, respectively, and the location of the fifth disulfide bond is indicated by a dashed red line. This figure was produced with MOLMOL (*28*).

protein stabilization by forming salt bridges or hydrogen bonds (*38*). However, the semiconserved threonine residue as a partner for the glutamate has not been described so far.

In several plant defensins, other residues participate in stabilizing interactions between the α-helix and strand β1 and the conserved hydrogen bond forms the core of a more extended network of hydrogen bonds and/or salt bridges between residues on the α-helix and strand β1. Although not a plant defensin, the prototype for such a network is drosomycin (Figure 5, top right) (*37, 38*). Here the role of the threonine is played by Arg6 (residue B) which forms salt bridges or hydrogen bonds with both Glu26 (residue A) and Glu25 (residue A′) (Figure 5, top right). Glu26 in turn

seems to be able to maintain hydrogen bonds with the semiconserved residue Ser4. The substitution of the otherwise prevalent threonine for arginine in drosomycin might explain why the contribution of this residue has not been described so far.

A second example is Ah-AMP1 (Figure 5, middle right) (*35*), where apart from Glu28 (residue A) and Thr9 (residue B), residues Gln8 and Arg5 on strand β1 as well as Gln23 on the α-helix participate in what is the most extensive hydrogen bond network of all plant defensins between the α-helix and strand β1.

An additional semiconserved residue deemed to be involved in protein stabilization is a serine at position 7

(numbering relative to NaD1) (*4, 5, 9*). In some plant defensins (e.g., NaD1, γ1-H, γ1-P, and drosomycin), the serine seems to participate in the network of hydrogen bonds between the α-helix and strand β1, in at least some models of the structural families (Figure 5). Often though (e.g., Ah-AMP1 and Rs-AFP1), the serine does not contribute to the hydrogen bond network (Figure 5, middle and bottom right) but rather is found to point toward a small internal cavity, which could contain one or two water molecules that could be essential for protein stability (*37, 38*). It has previously been suggested (*38*) that the serine (Ser7 in NaD1) is likely to play an important role in protein structure stabilization or in the protein folding pathway. In other cases (e.g., PhD1 and Psd1), the serine is replaced with other amino acids.

Interestingly, in PhD1 the conserved serine and glutamic acid residues are replaced with Cys7 and Ala27, respectively (Figure 5, middle left). These replacements are a direct consequence of the presence of the fifth disulfide bridge between Cys7 and Cys23 in PhD1. Ser7 is replaced because Cys7 forms part of this disulfide bond. Ala27 is present due to steric constraints, since there is not enough space for a glutamic acid next to the disulfide bond in PhD1. Nevertheless, PhD1 still contains the conserved hydrogen bond. Instead of Glu27 (which has been replaced with Ala27), the role of residue A is fulfilled by Lys26, which maintains a hydrogen bond with Thr9 (Figure 5, middle left). The same holds true for Psd1 (*36*) (Figure 5, bottom left), where residue A is replaced with Ala28. Instead, a hydrogen bond with Thr9 (residue B) is maintained by Lys27, which takes over the role of residue A from Ala28. It appears that the role of residue A is taken over by the preceding residue (termed residue A′) whenever residue A itself is missing so that the conserved hydrogen bond is always present. It is thus tempting to speculate that the conserved hydrogen bond is important for the stability or function of plant defensins and that this functional importance is the reason for the conservation of the threonine and the glutamic acid.

The importance of the conserved hydrogen bond for the function of plant defensins is further highlighted by the fact that mutation of Thr10 (residue B) to glycine, or mutation of Leu28 or Phe49, each of which is next to Glu27 (residue A), to an arginine results in a dramatic loss of activity in Rs-AFP2 (*39*). All these mutations are likely to disrupt the hydrogen bond between the threonine and the glutamic acid based on electrostatic considerations.

How is the fifth disulfide bond of PhD1 accommodated by the protein? The residues in all previously described structures of plant defensins, which are on the same sequential position as the two cysteines that form the fifth disulfide bond in PhD1, are close to each other in the structures (Figure 5). One half of the fifth disulfide bond in PhD1 is substituted with a semiconserved serine at position 7 in other plant defensins (numbering according to PhD1). As mentioned before, in most plant defensins, this residue points toward the interior of the protein and could be important for protein stability (*37, 38*). In addition, the serine has nearly the same steric requirements as a cysteine residue. The other half of the fifth disulfide bridge is Cys23. In other plant defensins, this is either a hydrophobic/aromatic residue (Val in drosomycin, γ1-H, and γ1-P, Ala in NaD1, and His in Psd1) that maintains interaction with the hydrophobic core of the protein or a polar residue (Gln in Rs-AFP1 and Ah-

AMP1) that contributes to the hydrogen bond network between the α-helix and strand β1. In both cases, the original residues have roughly the same steric requirements as a cysteine. Thus, it is not surprising that the fifth disulfide bond in PhD1 is seamlessly accommodated within the structure of PhD1 and that this additional disulfide bond influences the orientation of the α-helix with respect to the β-sheet only slightly when compared with solution structures of other plant defensins. In addition, the fifth disulfide bond is likely to confer additional thermodynamic stability on PhD1, when it is compared to other plant defensins, by replacing the noncovalent hydrophobic interactions or hydrogen bonds between the involved residues with a covalent bond.

Interestingly, the fifth disulfide bond of PhD1 is adjacent to the hydrogen bond between the conserved threonine and glutamic acid residues of the other plant defensins. Therefore, the additional disulfide bond seems to reinforce this hydrogen bond (Figure 5), showing the importance of stabilizing interactions in this region of the structure of plant defensins. This notion is also highlighted by the fact that most other plant defensins have a more extensive network of hydrogen bonds and/or salt bridges between the α-helix and strand β1 than PhD1, as discussed above. It appears that the fifth disulfide bond sufficiently stabilizes the protein to make part of the hydrogen bond network dispensable, thus playing an intricate role in the stabilization of the protein in a manner that is complementary to those of other plant defensins.

REFERENCES

1. Rao, A. G. (1995) Antimicrobial peptides, *Mol. Plant−Microbe Interact. 8*, 6−13.
2. Broekaert, W. F., Cammue, B. P. A., De Bolle, M. F. C., Thevissen, K., De Samblanx, G. W., and Osborn, R. W. (1997) Antimicrobial Peptides from Plants, *Crit. Rev. Plant Sci. 16*, 297−323.
3. Garcia-Olmedo, F., Molina, A., Alamillo, J. M., and Rodriguez-Palenzuela, P. (1988) Plant defense peptides, *Biopolymers 47*, 479−491.
4. Broekaert, W. F., Terras, F. R. G., Cammue, B. P. A., and Osborn, R. W. (1995) Plant defensins: novel antimicrobial peptides as components of the host defense system, *Plant Physiol. 108*, 1353−1358.
5. Lay, F. T., Schirra, H. J., Scanlon, M. J., Anderson, M. A., and Craik, D. J. (2003) The three-dimensional solution structure of NaD1, a new floral defensin from *Nicotiana alata* and its application to a homology model of the crop defense protein alfAFP, *J. Mol. Biol. 325*, 175−188.
6. Osborn, R. W., De Samblanx, G. W., Thevissen, K., Goderis, I., Torrekens, S., Van Leuven, F., Attenborough, S., Rees, S. B., and Broekaert, W. F. (1995) Isolation and characterisation of plant defensins from seeds of Asteraceae, Fabaceae, Hippocastanaceae and Saxifragaceae, *FEBS Lett. 368*, 257−262.
7. Thevissen, K., Ghazi, A., De Samblanx, G. W., Brownlee, C., Osborn, R. W., and Broekaert, W. F. (1996) Fungal membrane responses induced by plant defensins and thionins, *J. Biol. Chem. 271*, 15018−15025.
8. Cornet, B., Bonmatin, J. M., Hetru, C., Hoffmann, J. A., Ptak, M., and Vovelle, F. (1995) Refined three-dimensional solution structure of insect defensin A, *Structure 3*, 435−448.
9. Bruix, M., Jimenez, M. A., Santoro, J., Gonzalez, C., Colilla, F. J., Mendez, E., and Rico, M. (1993) Solution structure of γ1-H and γ1-P thionins from barley and wheat endosperm determined by ^{1}H NMR: a structural motif common to toxic arthropod proteins, *Biochemistry 32*, 715−724.
10. Lay, F. T., Brugliera, F., and Anderson, M. A. (2003) Isolation and properties of floral defensins from ornamental tobacco and petunia, *Plant Physiol. 131*, 1283−1293.

11. Marion, D., and Wüthrich, K. (1983) Application of phase sensitive two-dimensional correlated spectroscopy (COSY) for measurements of ^{1}H-^{1}H-spin coupling constants in proteins, *Biochem. Biophys. Res. Commun. 113*, 967−974.

12. Sklenar, V., Piotto, M., Leppik, R., and Saudek, V. (1993) Gradient-tailored water suppression for H-1-N-15 HSQC experiments optimized to retain full sensitivity, *J. Magn. Reson., Ser. A 102*, 241−245.

13. Bax, A., and Davies, D. G. (1985) MLEV-17 based two-dimensional homonuclear magnetisation transfer spectroscopy, *J. Magn. Reson. 65*, 355−360.

14. Rance, M., Sørensen, O. W., Bodenhausen, G., Wagner, G., Ernst, R. R., and Wüthrich, K. (1983) Improved spectral resolution in COSY ^{1}H NMR spectra of proteins via double quantum filtering, *Biochem. Biophys. Res. Commun. 117*, 479−485.

15. Braunschweiler, L., and Ernst, R. R. (1983) Coherence transfer by isotropic mixing: application to proton correlation spectroscopy, *J. Magn. Reson. 53*, 521−528.

16. Kumar, A., Ernst, R. R., and Wüthrich, K. (1980) A two-dimensional nuclear Overhauser enhancement (2D NOE) experiment for the elucidation of complete proton−proton cross-relaxation networks in biological macromolecules, *Biochem. Biophys. Res. Commun. 95*, 1−6.

17. Griesinger, C., Sørensen, O. W., and Ernst, R. R. (1985) Two-dimensional correlation of connected MR transitions, *J. Am. Chem. Soc. 107*, 6394−6396.

18. Schleucher, J., Schwendiger, M., Sattler, M., Schmidt, P., Schedletzky, P., Glaser, S. J., Sørensen, O. W., and Griesinger, C. (1994) A general enhancement scheme in heteronuclear multidimensional NMR employing pulsed field gradients, *J. Biomol. NMR 4*, 301−306.

19. Cieslar, C., Ross, A., Zink, T., and Holak, T. A. (1993) Efficiency in multidimensional NMR by optimized recording of time point-phase pairs in evolution periods and their selective linear transformation, *J. Magn. Reson., Ser. B 101*, 97−101.

20. Wüthrich, K. (1986) *NMR of Proteins and Nucleic Acids*, Wiley-Interscience, New York.

21. Wüthrich, K., Tun-Kyi, A., and Schwyzer, R. (1972) Manifestation in the ^{13}C-NMR spectra of two different molecular conformations of a cyclic pentapeptide, *FEBS Lett. 25*, 104−108.

22. Holak, T. A., Gondol, D., Otlewski, J., and Wilusz, T. (1989) Determination of the complete three-dimensional structure of the trypsin inhibitor from squash seeds in aqueous solution by nuclear magnetic resonance and a combination of distance geometry and dynamical simulated annealing, *J. Mol. Biol. 210*, 635−648.

23. Pardi, A., Billeter, M., and Wüthrich, K. (1984) Calibration of the angular dependence of the amide proton-C$^\alpha$ proton coupling constants, $^3J_{HN\alpha}$ in a globular protein, *J. Mol. Biol. 180*, 741−751.

24. Wagner, G., Braun, W., Havel, T. F., Schaumann, T., Go, N., and Wüthrich, K. (1987) Protein structures in solution by nuclear magnetic resonance and distance geometry. The polypeptide fold of the basic pancreatic trypsin inhibitor determined using two different algorithms, DISGEO and DISMAN, *J. Mol. Biol. 196*, 611−639.

25. Brünger, A. T. (1992) *X-PLOR Version 3.1 Manual*, Yale University Press, New Haven, CT.

26. Brünger, A. T., Adams, P. D., Clore, G. M., DeLano, W. L., Gros, P., GrosseKunstleve, R. W., Jiang, J. S., Kuszewski, J., Nilges, M., Pannu, N. S., Read, R. J., Rice, L. M., Simonson, T., and Warren, G. L. (1998) Crystallography and NMR system (CNS): A new software system for macromolecular structure determination, *Acta Crystallogr. D54*, 905−921.

27. Linge, J. P., and Nilges, M. (1999) Influence of non-bonded parameters on the quality of NMR structures: A new force-field for NMR structure determination, *J. Biomol. NMR 13*, 51−59.

28. Koradi, R., Billeter, M., and Wüthrich, K. (1996) MOLMOL: a program for display and analysis of macromolecular structures, *J. Mol. Graphics 14*, 51−55.

29. Hutchinson, E. G., and Thornton, J. M. (1996) PROMOTIF: a program to identify and analyse structural motifs in proteins, *Protein Sci. 5*, 212−220.

30. Laskowski, R. A., Rullman, J. A., MacArthur, M. W., Kaptein, R., and Thornton, J. M. (1996) AQUA and PROCHECK-NMR: programs for checking the quality of protein structures solved by NMR, *J. Biomol. NMR 8*, 477−486.

31. Richardson, J. S., and Richardson, D. C. (1989) in *Prediction of Protein Structure and the Principles of Protein Conformation* (Fasman, G. D., Ed.) pp 1−98, Plenum Press, London.

32. Fant, F., Vranken, W. F., Martins, J. C., and Borremans, F. A. M. (1998) Determination of the three-dimensional solution structure of *Raphanus sativus* antifungal protein 1 by ^{1}H NMR, *J. Mol. Biol. 279*, 257−270.

33. Kobayashi, Y., Takashima, H., Tamaoki, H., Kyogoku, Y., Lambert, P., Kuroda, H., Chino, N., Watanabe, T. X., Kimura, T., Sakakibara, S., and Moroder, L. (1991) The cystine-stabilized α-helix: a common structural motif of ion-channel blocking neurotoxic peptides, *Biopolymers 31*, 1213−1220.

34. Sigrist, C. J., Cerutti, L., Hulo, N., Gattiker, A., Falquet, L., Pagni, M., Bairoch, A., and Bucher, P. (2002) PROSITE: a documented database using patterns and profiles as motif descriptors, *Briefings Bioinf. 3*, 265−274.

35. Fant, F., Vranken, W. F., and Borremans, F. A. M. (1999) The three-dimensional solution structure of *Aesculus hippocastanum* antimicrobial protein 1 determined by ^{1}H nuclear magnetic resonance, *Proteins 37*, 388−403.

36. Almeida, M. S., Cabral, K. M., Kurtenbach, E., Almeida, F. C., and Valente, A. P. (2002) Solution structure of *Pisum sativum* defensin 1 by high-resolution NMR: plant defensins, identical backbone with different mechanisms of action, *J. Mol. Biol. 315*, 749−757.

37. Landon, C., Sodano, P., Hetru, C., Hoffmann, J. A., and Ptak, M. (1997) Solution structure of drosomycin, the first inducible antifungal protein from insects, *Protein Sci. 6*, 1878−1884.

38. Landon, C., Pajon, A., Vovelle, F., and Sodano, P. (2000) The active site of drosomycin, a small insect antifungal protein, delineated by comparison with the modeled structure of Rs-AFP2, a plant antifungal protein, *J. Pept. Res. 56*, 231−238.

39. De Samblanx, G. W., Goderis, I. J., Thevissen, K., Raemaekers, R., Fant, F., Borremans, F., Acland, D. P., Osborn, R. W., Patel, S., and Broekaert, W. F. (1997) Mutational analysis of a plant defensin from radish (*Raphanus sativus L.*) reveals two adjacent sites important for antifungal activity, *J. Biol. Chem. 272*, 1171−1179.

40. Bruix, M., Gonzalez, C., Santoro, J., Soriano, F., Rocher, A., and Mendez, E. (1995) ^{1}H-NMR studies on the structure of a new thionin from barley endosperm, *Biopolymers 36*, 751−763.

41. Bloch, C., Jr., Patel, S. U., Baud, F., Zvelebil, M. J., Carr, M. D., Sadler, P. J., and Thornton, J. M. (1998) ^{1}H NMR structure of an antifungal gamma-thionin protein SIα1: similarity to scorpion toxins, *Proteins 32*, 334−349.

42. Wishart, D. S., Sykes, B. D., and Richards, F. M. (1992) The chemical shift index: a fast and simple method for the assignment of protein secondary structure through NMR spectroscopy, *Biochemistry 31*, 1647−1651.

43. Nicholls, A., Sharp, K. A., and Honig, B. (1991) Protein folding and association insights from the interfacial and thermodynamic properties of hydrocarbons, *Proteins 11*, 281−296.